

Cite this: *RSC Adv.*, 2017, 7, 40829

Received 19th July 2017  
Accepted 16th August 2017  
DOI: 10.1039/c7ra07938a  
[rsc.li/rsc-advances](http://rsc.li/rsc-advances)

# An indolizine–rhodamine based FRET fluorescence sensor for highly sensitive and selective detection of Hg<sup>2+</sup> in living cells†

Ruixue Ji, Aikun Liu, Shili Shen, Xiaoqun Cao,  Fei Li and Yanqing Ge \*

An indolizine–rhodamine-based ratiometric fluorescent probe was designed and successfully synthesized. The probe shows a large Stokes shift (204 nm), high sensitivity and high selectivity. The detection limit was calculated to be as low as 8.76 nM. The probe could quickly (5 min) detect Hg<sup>2+</sup> over a wide pH range from 5 to 10. Furthermore, it could be used for imaging Hg<sup>2+</sup> in living cells.

## Introduction

Mercury ions, as a dangerous and widespread global pollutant, can easily pass through skin, respiratory and gastrointestinal tissues into the human body, and damage the central nervous and endocrine systems. Therefore, accurate, rapid and cheap detection of mercury ions *in vitro* and *in vivo* with high selectivity and sensitivity is highly demanded.<sup>1–3</sup>

Several methods have been developed to monitor concentration levels of mercury such as atomic absorption spectroscopy, inductively coupled plasma-atomic emission spectrometry, gas chromatography-inductively coupled plasma-mass spectrometry, atomic fluorescence spectrometry (AFS), and reversed-phase high-performance liquid chromatography.<sup>4,5</sup> These methods provide limits of detection at parts-per-billion level. However, their excellent performance is achieved at the expenses of elaborate and time-consuming sample preparation and preconcentration procedures. Most importantly, they cannot be used to detect Hg<sup>2+</sup> in living cells. In general, fluorescence is a powerful optical analytical technique suitable for detecting low concentration of analytes.<sup>2</sup>

Since Tae reported the first Hg<sup>2+</sup> probe based on rhodamine derivative,<sup>6</sup> a number of intensity-based Hg<sup>2+</sup> probes were synthesized. However, a major limitation of these simple “turn off” or “turn on” probes is that variations in probe concentration, probe environment, or excitation intensity may influence the fluorescence intensity measurements. Ratiometric sensors can eliminate most or all ambiguities by selfcalibration of two emission bands.<sup>7–10</sup>

Most ratiometric probes can be designed to function the following two mechanisms: intramolecular charge transfer (ICT) and Förster resonance energy transfer (FRET). However,

some ICT-type ratiometric fluorescent probes have very broad emission spectra, which often lead to serious overlap in the emission peaks before and after interaction with target analytes. The above problems can be avoided by using a FRET-based sensor for which the single excitation wavelength of a donor fluorophore results in emission of the acceptor at a longer wavelength.<sup>11–30</sup>

In order to further improve biocompatibility, accuracy and detection efficiency of a probe, herein we present an indolizine–rhodamine FRET system **TMUHg-2** as a ratiometric and intracellular Hg<sup>2+</sup> sensor. A leuco-rhodamine derivative was chosen as a sensitive and selective chemosensor for Hg<sup>2+</sup> ions. A highly efficient ring-opening reaction induced by Hg<sup>2+</sup> generates the long-wavelength rhodamine fluorophore which can act as the energy acceptor. Indolizine, which was successfully synthesized *via* a novel tandem reaction by our group,<sup>31,32</sup> was chosen as the energy donor because its max emission wavelength matches well with the absorption spectrum of rhodamine (Fig. S1†). As expected, **TMUHg-2** could quickly (5 min) detect Hg<sup>2+</sup> with high sensitivity and selectivity in a wide pH range from 5 to 10. The detection limit of 8.76 nM was achieved. More importantly, **TMUHg-2** could be used for imaging Hg<sup>2+</sup> in living cells.

## Experimental

### Materials and equipments

UV-vis spectra were measured with a Hitachi U-4100 spectrophotometer. Thin-layer chromatography involved silica gel 60 F<sub>254</sub> plates (Merck KGaA) and column chromatography involved silica gel (mesh 200–300). All of the pH values were measured with a PHS-3C pH meter. Quartz cuvettes with a 1 cm path length and 3 mL volume were used in fluorescence and UV-vis spectrum measurements. Dry white wine (Changyu Pioneer Wine Company Limited, Yantai) were used with no pretreatment. UV-vis spectra and fluorescence spectra were recorded on a U-3900 UV-vis spectrometer (Hitachi) and RF-5301PC luminescence spectrophotometer (Shimadzu) at

School of Chemistry and Pharmaceutical Engineering, Taishan Medical University, Taian 271000, PR China. E-mail: [geyanqing2016@126.com](mailto:geyanqing2016@126.com); Tel: +86-538-6236195

† Electronic supplementary information (ESI) available: <sup>1</sup>H NMR, <sup>13</sup>C NMR and MS spectra of probe, and additional cell images. See DOI: 10.1039/c7ra07938a

room temperature, respectively.  $^1\text{H}$  NMR and  $^{13}\text{C}$  NMR spectra were measured on a Bruker Avance 400 (400 MHz) spectrometer ( $\text{CDCl}_3$  as solvent and tetramethylsilane (TMS) as an internal standard). HRMS spectra were recorded on a Q-TOF6510 spectrophotograph (Agilent). All reagents and solvents were purchased from commercial sources and used without further purification. The solutions of metal ions were prepared from chloridized salts which were dissolved in deionized water. Deionized water was used throughout the process of absorption and fluorescence determination.

### Cell culture and imaging

Glioma cells (The department of pharmacology of Taishan Medical University, China, provided the cell line.) were cultured in RPMI-1640 containing 10% fetal bovine serum at  $37^\circ\text{C}$  in a 5%  $\text{CO}_2$ /95% air incubator. For living cells imaging experiments, the growth medium was removed and replaced with RPMI-1640 without FBS. The cells were treated and incubated with  $2\text{ }\mu\text{M}$  of **TMUHg-2** at  $37^\circ\text{C}$  under 5%  $\text{CO}_2$  for 1 h. The cells were washed three times with PBS and then cell images were obtained *via* a confocal microscope from FV1000 (Olympus) at excitation of 405 nm.

Compound 1 and 2 were synthesized according to the literature.<sup>31–34</sup>

### Synthesis of compound 3

Compound 1 (203 mg, 1 mmol) was dissolved in  $\text{CH}_2\text{Cl}_2$  (20 mL), and then EDC (288 mg, 1.5 mmol) and DMAP (30 mg, 0.2 mmol) were added. Subsequently, compound 2 (470 mg, 1 mmol) was added, and the reaction mixture was stirred at room temperature for 6 h. Then the solvent was removed under reduced pressure to afford crude compound 3, which was purified on a silica gel column ( $\text{C}_2\text{H}_5\text{OH} : \text{CH}_2\text{Cl}_2 = 1 : 200$ ) to afford pure compound 3 (491 mg, 75%).  $^1\text{H}$  NMR (400 MHz,  $\text{CDCl}_3$ ),  $\delta$  7.95–7.91 (m, 2H), 7.85 (s, 1H), 7.53 (s, 1H), 7.47 (m, 2H), 7.08 (m, 1H), 6.95 (s, 1H), 6.68 (m, 2H), 6.56 (s, 2H), 6.45 (m, 2H), 6.32 (m, 1H), 3.81 (s, 4H), 3.66 (s, 2H), 3.35 (q,  $J = 8.0\text{ Hz}$ , 4H), 3.27 (s, 4H), 2.57 (s, 3H), 1.17 (t,  $J = 8.0\text{ Hz}$ , 6H).  $^{13}\text{C}$  NMR (100 MHz,  $\text{CDCl}_3$ ),  $\delta$  194.62, 168.81, 166.21, 153.51, 151.63, 151.17, 148.95, 132.65, 131.46, 129.84, 129.60, 128.37, 128.16, 128.05, 125.59, 125.01, 123.74, 123.10, 120.54, 116.27, 112.18, 111.84, 110.06, 108.30, 104.11, 103.13, 102.55, 97.88, 65.51, 48.78, 44.37, 27.74, 12.53.

### Synthesis of the probe TMUHg-2

Compound 3 (131 mg, 0.2 mmol) in DMF (1.5 mL) was added to a solution of phenyl isothiocyanate (0.1 mL, 0.65 mmol) in DMF (1.5 mL). The reaction mixture was stirred for 12 h at room temperature. After the solvent was evaporated under reduced pressure, the crude product was column chromatographed on silica gel ( $\text{C}_2\text{H}_5\text{OH} : \text{CH}_2\text{Cl}_2 = 1 : 200$ ) to give the 80 mg (50%) of **TMUHg-2**. Mp:  $170\text{--}171^\circ\text{C}$ .  $^1\text{H}$  NMR (400 MHz,  $\text{CDCl}_3$ )  $\delta$  8.04 (d,  $J = 8.0\text{ Hz}$ , 1H), 7.93 (d,  $J = 8.0\text{ Hz}$ , 1H), 7.86 (s, 1H), 7.68 (m, 1H), 7.62 (m, 1H), 7.54 (s, 1H), 7.48 (s, 1H), 7.19 (m, 2H), 7.11 (m, 1H), 7.05 (d,  $J = 8.0\text{ Hz}$ , 2H), 6.96 (s, 1H), 6.89 (s, 1H), 6.69 (m, 2H), 6.53 (m, 3H), 6.44 (s, 1H), 6.30 (d,  $J = 8.0\text{ Hz}$ , 1H), 3.80

(s, 4H), 3.34 (m, 4H), 3.26 (s, 4H), 2.58 (s, 3H), 1.15 (t,  $J = 8.0\text{ Hz}$ , 6H).  $^{13}\text{C}$  NMR (100 MHz,  $\text{CDCl}_3$ )  $\delta$  194.7, 168.8, 162.5, 154.1, 153.9, 152.1, 149.6, 149.4, 134.4, 131.5, 129.6, 129.3, 129.0, 128.4, 127.6, 125.6, 125.0, 124.7, 124.0, 120.6, 116.3, 112.4, 111.9, 108.7, 103.4, 102.6, 98.2, 66.8, 48.5, 44.4, 27.8, 12.5. HRMS: 790.3168 ( $[\text{M} + \text{H}]^+$ ); calcd for  $\text{C}_{46}\text{H}_{44}\text{N}_7\text{O}_4\text{S}$ : 790.3175.

## Results and discussion

### Synthesis of the probe TMUHg-2

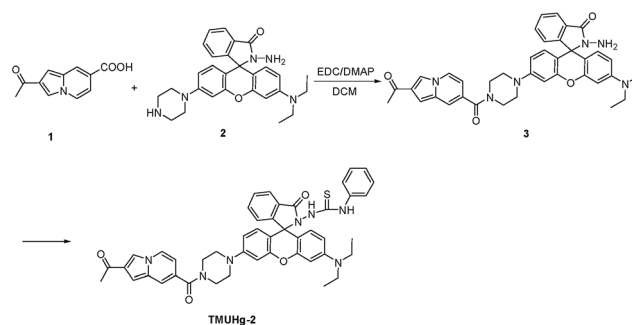
The synthetic route to access probe **TMUHg-2** is shown in Scheme 1. The reaction of Rhodamine B hydrazide 3 and phenyl isothiocyanate in DMF afforded probe **TMUHg-2** as pink powder in 50% yield. The probe **TMUHg-2** was characterized by  $^1\text{H}$  NMR,  $^{13}\text{C}$  NMR and HRMS (see ESI†).

The Fig. 1 demonstrated that **TMUHg-2** was characteristic of high selectivity toward  $\text{Hg}^{2+}$  over other competitive metal ions and could serve as a “naked-eye” chemodosimeter. The competitive cations did not lead to any significant absorption changes in the visible region. However, a clear color change from colourless to pink was observed upon the addition of 1 equiv. of  $\text{Hg}^{2+}$ .

The absorption spectra of **TMUHg-2** with varying  $\text{Hg}^{2+}$  concentrations (0–5 equiv.) in  $\text{C}_2\text{H}_5\text{OH}/\text{water}$  (2/8, v/v) were also recorded to further investigate the interaction of **TMUHg-2** and  $\text{Hg}^{2+}$  (Fig. S2†). When  $\text{Hg}^{2+}$  was added to the solution of **TMUHg-2** (10  $\mu\text{M}$ ), a new absorption band centered at 564 nm appeared with increasing intensity, which could be ascribed to the formation of the ring-opened form of **TMUHg-2**.

### Fluorescence spectra

The selectivity of **TMUHg-2** for  $\text{Hg}^{2+}$  was further observed in the fluorescent spectra. **TMUHg-2** alone exhibited an emission of the indolizine centered about 434 nm when excited at 380 nm indicating the spirocyclic form of rhodamine moiety (Fig. 2). Addition of 1 equiv. of  $\text{Hg}^{2+}$  into the solution immediately resulted in a significant enhancement of fluorescent intensity at 584 nm and an obvious decrease of fluorescent intensity at 434 nm. Other competitive cations did not lead to any significant fluorescent changes. The phenomenon suggested that the Rhodamine was induced to be transformed into the open-ring structure from the spirocyclic form by  $\text{Hg}^{2+}$ .



Scheme 1 The synthesis of probe **TMUHg-2**.



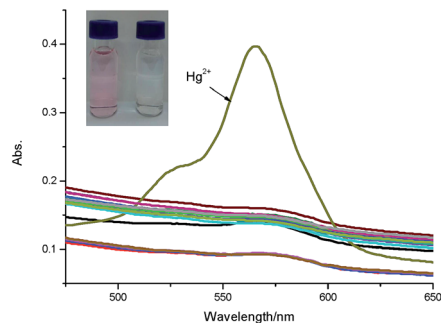


Fig. 1 Absorbance spectra of **TMUHg-2** (10  $\mu\text{M}$ ) in the absence and presence of 1 equiv. of different metal ions in  $\text{C}_2\text{H}_5\text{OH}/\text{H}_2\text{O}$  (2/8, v/v) solution.

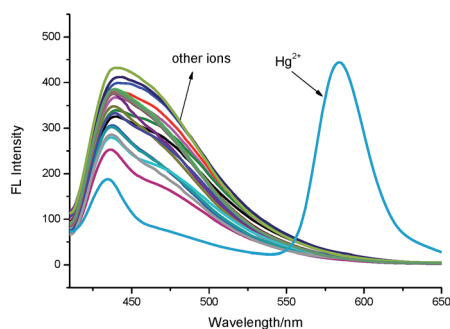


Fig. 2 Fluorescence spectra of **TMUHg-2** (1  $\mu\text{M}$ ) in the absence and presence of 1 equiv. of different metal ions in  $\text{C}_2\text{H}_5\text{OH}/\text{H}_2\text{O}$  (2/8, v/v) solution ( $\lambda_{\text{ex}}$  = 380 nm, slit = 15 nm/10 nm).

The fluorescence titration of **TMUHg-2** was recorded as shown in Fig. 3. With the increasing concentrations of  $\text{Hg}^{2+}$ , the intensity of fluorescence at 434 nm gradually decreased, while the band centering around 584 nm became prominent. The Stoke shift was 204 nm and the two emission peaks were well separated (150 nm). The results demonstrated that the developed FRET system effectively avoided the emission spectra overlap and ensured accuracy and high resolution in determining of  $\text{Hg}^{2+}$ . More importantly, the fluorescence intensity ratio ( $I_{584}/I_{434}$ ) increased dramatically with increasing amount of  $\text{Hg}^{2+}$ , which changed about 54.6 times (from 0.046 to 2.51) when the concentration of  $\text{Hg}^{2+}$  was increased from 0 to 1  $\mu\text{M}$ .

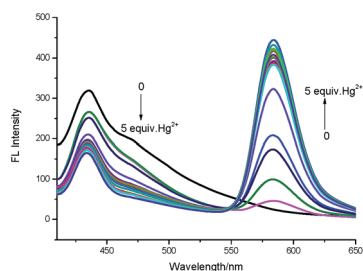


Fig. 3 Fluorescence spectra of **TMUHg-2** (1  $\mu\text{M}$ ) in response to  $\text{Hg}^{2+}$  (0.0–5.0 equiv.) in  $\text{C}_2\text{H}_5\text{OH}/\text{H}_2\text{O}$  (2/8, v/v) solution ( $\lambda_{\text{ex}}$  = 380 nm, slit = 15 nm/10 nm).

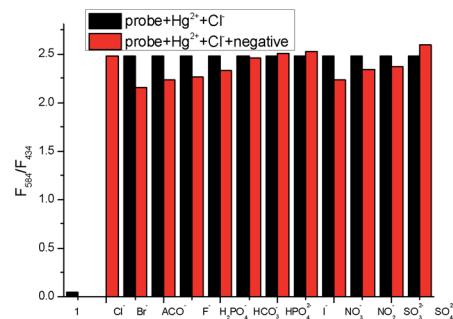


Fig. 4 The ratiometric fluorescence responses  $F_{584}/F_{434}$  of **TMUHg-2** (1  $\mu\text{M}$ ) upon the addition of 1  $\mu\text{M}$   $\text{HgCl}_2$  in the presence of 1  $\mu\text{M}$  background anions in  $\text{C}_2\text{H}_5\text{OH}/\text{H}_2\text{O}$  (2/8, v/v) solution.

There was a good linear relationship (Fig. S3†) in the concentration range from 0.02  $\mu\text{M}$  to 0.10  $\mu\text{M}$  of  $\text{Hg}^{2+}$  ( $R_2 = 0.9858$ ) and the detection limit was calculated to be as low as 8.76 nM. Also, it was investigated that the fluorescence responded in the presence of various coexistent anions (Fig. 4). It is gratifying to note that all the tested anions have no obvious interference with the fluorescence response of **TMUHg-2** toward  $\text{Hg}^{2+}$ . Moreover, the competitive experiments of the background metal ions were also studied. As shown in Fig. 5, the background metal ions showed very low interference with the detection.

### Kinetic study

A time course of the fluorescence response of **TMUHg-2** upon addition of  $\text{Hg}^{2+}$  is shown in Fig. 6. The kinetics of fluorescence intensity ratiometric changes of  $F_{584}/F_{434}$  indicated that it could be complete in 5 min so that it could be used as a ratiometric fluorescent probe for the fast detection of  $\text{Hg}^{2+}$ .

### Effect of pH

In order to find a suitable pH span in which **TMUHg-2** can selectively detect  $\text{Hg}^{2+}$  efficiently, the acid titration experiments were performed. As illustrated in Fig. 7, the free probe and the probe in the presence of  $\text{Hg}^{2+}$  did not show obvious changes of

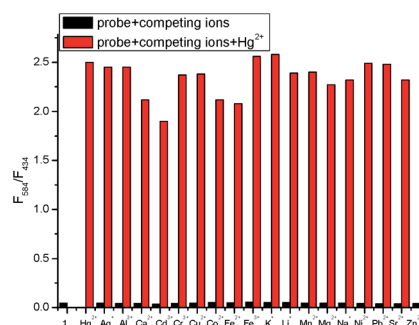


Fig. 5 Metal-ion selectivity of **TMUHg-2** in  $\text{C}_2\text{H}_5\text{OH}/\text{H}_2\text{O}$  (2/8, v/v) solution. The black bars represent the fluorescence emission ratio ( $F_{584}/F_{434}$ ) of a solution of **TMUHg-2** (1  $\mu\text{M}$ ) and 1 equiv. of other metal ions. The red bars show the  $F_{584}/F_{434}$  ratio after the addition of 1 equiv. of  $\text{Hg}^{2+}$  to the solution containing **TMUHg-2** (1  $\mu\text{M}$ ) and different metal ions (1  $\mu\text{M}$ ) ( $\lambda_{\text{ex}}$  = 380 nm, slit = 15 nm/10 nm).



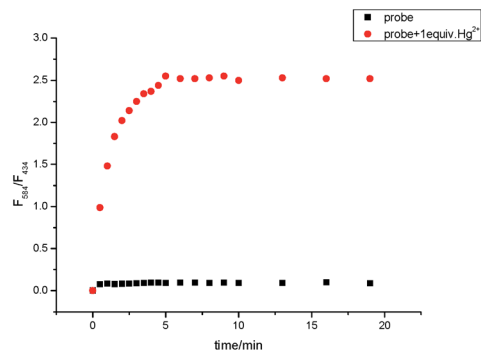


Fig. 6 Time dependent increase of **TMUHg-2** (1  $\mu$ M) fluorescence intensities after addition of various amounts of  $\text{Hg}^{2+}$  in  $\text{C}_2\text{H}_5\text{OH}/\text{H}_2\text{O}$  (2/8, v/v) solution ( $\lambda_{\text{ex}}$  = 380 nm, slit = 15 nm/10 nm).

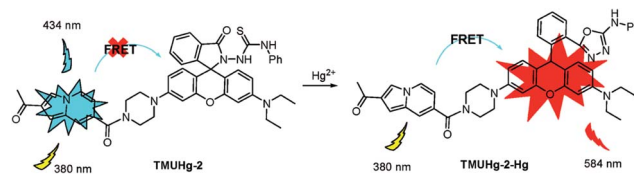
the fluorescence intensity ratio ( $F_{584}/F_{434}$ ) between pH 5.0 and 10.0, suggesting that the probe **TMUHg-2** might be used to detect  $\text{Hg}^{2+}$  in approximate physiological conditions.

### Mechanism

Based on the previous work,<sup>6</sup> we envisioned that probe **TMUHg-2** is in the spiro ring-closing state and the FRET must be off before reacting with  $\text{Hg}^{2+}$ . Addition of  $\text{Hg}^{2+}$  may induce the rhodamine acceptor to be in the ring-opened form *via*  $\text{Hg}^{2+}$ -promoted reaction of thiosemicarbazides to form 1,3,4-oxadiazoles and the FRET must be on (Scheme 2). The form of **TMUHg-2-Hg**<sup>2+</sup> was also confirmed by HRMS analysis (Fig. S13 and S14<sup>†</sup>). When  $\text{HgCl}_2$  was added to **TMUHg-2** in  $\text{CH}_3\text{OH}$ , the peak of [**TMUHg-2** +  $\text{H}$ ]<sup>+</sup> (790.3168) disappeared, and at the same time, a new peak of 756.3332 appeared, which suggested the formation of the compound [**TMUHg-2-Hg** –  $\text{H}$ ]<sup>+</sup>.

### Cell imaging

The MTT assays (Fig. S4<sup>†</sup>) suggest that the ratiometric probe has low cytotoxicity to the cells. In light of the high sensitivity, selectivity and low cytotoxicity of **TMUHg-2** for detecting  $\text{Hg}^{2+}$ , the probe was applied to ratiometric fluorescence imaging in living cells. Glioma cells were incubated with only **TMUHg-2**



Scheme 2 Proposed sensing mechanism of **TMUHg-2** with  $\text{Hg}^{2+}$ .

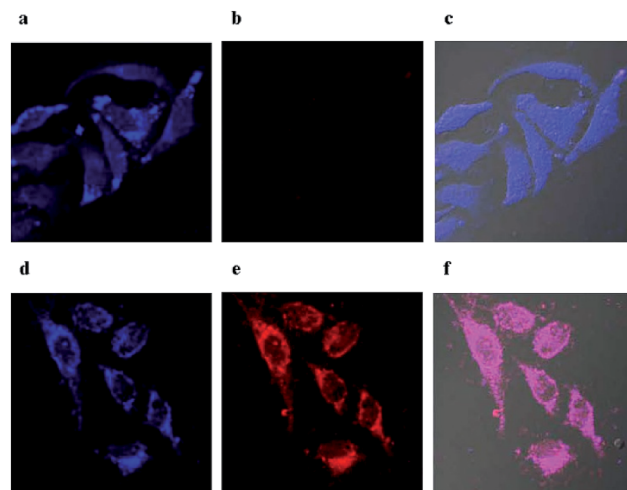


Fig. 8 Images of glioma cells treated with the probe. Fluorescence image of glioma cells incubated with probe (2  $\mu$ M) for 2 h ((a) the blue channel, (b) the red channel); (c) overlay image of (a and b) and bright field; fluorescence image of glioma cells incubated with probe (2  $\mu$ M) for 2 h and then further incubated with  $\text{Hg}^{2+}$  (2  $\mu$ M) for 30 min ((d) the blue channel, (e) the red channel); (f) overlay image of (d and e) and bright field.

(2  $\mu$ M) for 2 h at 37  $^{\circ}\text{C}$ , and the cells showed strong fluorescence in the blue channel (Fig. 8a) and weak fluorescence in the red channel (Fig. 8b). However, when cells were incubated with **TMUHg-2** for 2 h, then incubated with  $\text{Hg}^{2+}$  for 30 min, the bright blue fluorescence darkened (Fig. 8d) and the faint red fluorescence brightened (Fig. 8e).

## Conclusions

In summary, a new indolizine–rhodamine-based  $\text{Hg}^{2+}$  ratiometric fluorescent probe was designed and successfully synthesized. The probe **TMUHg-2** showed high selectivity and high sensitivity toward  $\text{Hg}^{2+}$ . The detection limit was calculated to be as low as 8.76 nM. It could quickly (5 min) detect  $\text{Hg}^{2+}$  over a wide pH range from 5 to 10. Remarkably, the novel ratiometric fluorescent probes exhibited a large Stokes shift (204 nm) which can avoid auto-fluorescence, serious self-quenching and fluorescence detection errors. Furthermore, the probe has been successfully used for recognition of  $\text{Hg}^{2+}$  in cells.

## Conflicts of interest

There are no conflicts to declare.

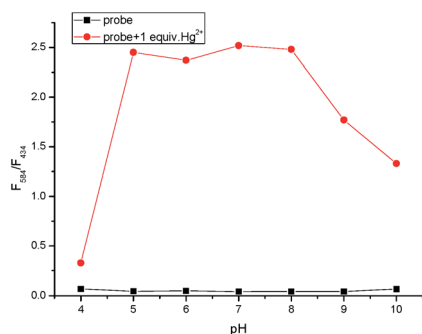


Fig. 7 The ratiometric fluorescence responses ( $F_{584}/F_{434}$ ) of free **TMUHg-2** (1  $\mu$ M) and in the presence of 1 equiv. of  $\text{Hg}^{2+}$  in  $\text{C}_2\text{H}_5\text{OH}/\text{H}_2\text{O}$  (2/8, v/v) solution with different pH conditions ( $\lambda_{\text{ex}}$  = 380 nm, slit = 15 nm/10 nm).





## Acknowledgements

This work was supported by the Natural Science Foundation of China (21602153), the Science Fund of Shandong Province for Excellent Young Scholars (ZR201702180206) and Higher Educational Science and Technology Program of Shandong Province (J13LM01).

## Notes and references

- 1 E. M. Nolan and S. J. Lippard, *Chem. Rev.*, 2008, **108**, 3443.
- 2 Y. M. Yang, Q. Zhao, W. Feng and F. Y. Li, *Chem. Rev.*, 2013, **113**, 192.
- 3 H. R. Yang, C. M. Han, X. J. Zhu, Y. Liu, K. Y. Zhang, S. J. Liu, Q. Zhao, F. Y. Li and W. Huang, *Adv. Funct. Mater.*, 2016, **26**, 1945.
- 4 J. L. Chen, A. F. Zheng, A. H. Chen, Y. C. Gao, C. Y. He, X. M. Kai, G. H. Wu and Y. C. Chen, *Anal. Chim. Acta*, 2007, **599**, 134.
- 5 K. H. Chu, Y. Zhou, Y. Fang, L. H. Wang, J. Y. Li and C. Yao, *Dyes Pigm.*, 2013, **98**, 339.
- 6 Y. K. Yang, K. J. Yook and J. Tae, *J. Am. Chem. Soc.*, 2005, **127**, 16760.
- 7 M. H. Lee, J. S. Kim and J. L. Sessler, *Chem. Soc. Rev.*, 2015, **44**, 4185.
- 8 J. L. Fan, M. M. Hu, P. Zhan and X. J. Peng, *Chem. Soc. Rev.*, 2013, **42**, 29.
- 9 L. Yuan, W. Y. Lin, K. B. Zheng and S. S. Zhu, *Acc. Chem. Res.*, 2013, **46**, 1462.
- 10 L. W. He, B. L. Dong, Y. Liu and W. Y. Lin, *Chem. Soc. Rev.*, 2016, **45**, 6449.
- 11 X. L. Zhang, Y. Xiao and X. H. Qian, *Angew. Chem., Int. Ed.*, 2008, **47**, 8025.
- 12 P. Wang, L. Y. Zhao, H. G. Shou, J. Y. Wang, P. L. Zheng, K. Jia and X. B. Liu, *Sens. Actuators, B*, 2016, **230**, 337.
- 13 M. Wang, J. Wen, Z. H. Qin and H. M. Wang, *Dyes Pigm.*, 2015, **120**, 208.
- 14 Y. Fang, Y. Zhou, J. Y. Li, Q. Q. Rui and C. Yao, *Sens. Actuators, B*, 2015, **215**, 350.
- 15 B. L. Dong, X. Z. Song, C. Wang, X. Q. Kong, Y. H. Tang and W. Y. Lin, *Anal. Chem.*, 2016, **88**, 4085.
- 16 D. D. Cheng, W. Q. Zhao, H. Z. Yang, Z. P. Huang, X. L. Liu and A. X. Han, *Tetrahedron Lett.*, 2016, **57**, 2655.
- 17 L. W. He, S. S. Zhu, Y. Liu, Y. N. Xie, Q. Y. Xu, H. P. Wei and W. Y. Lin, *Chem.-Eur. J.*, 2015, **21**, 12181.
- 18 L. W. He, X. L. Yang, Y. Liu and W. Y. Lin, *Anal. Methods*, 2016, **8**, 8022.
- 19 L. Yuan, W. Y. Lin, Y. N. Xie, B. Chen and S. S. Zhu, *J. Am. Chem. Soc.*, 2012, **134**, 1305.
- 20 Q. J. Ma, X. B. Zhang, X. H. Zhao, Z. Jin, G. J. Mao, G. L. Shen and R. Q. Yu, *Anal. Chim. Acta*, 2010, **663**, 85.
- 21 L. W. He, W. Y. Lin, Q. Y. Xu and H. P. Wei, *Chem. Commun.*, 2015, **51**, 1510.
- 22 Y. L. Liu, X. Lv, Y. Zhao, M. L. Chen, J. Liu, P. Wang and W. Guo, *Dyes Pigm.*, 2012, **92**, 909.
- 23 P. H. Xie, F. Q. Guo, L. Y. Wang, S. Yang, D. H. Yao and G. Y. Yang, *J. Fluoresc.*, 2015, **25**, 319.
- 24 D. D. Cheng, W. Q. Zhao, H. Z. Yang, Z. P. Huang, X. L. Liu and A. X. Han, *Tetrahedron Lett.*, 2016, **57**, 2655.
- 25 W. Y. Lin, X. W. Cao, Y. D. Ding, L. Yuan and L. L. Long, *Chem. Commun.*, 2010, **46**, 3529.
- 26 W. Y. Lin, X. W. Cao, Y. D. Ding, L. Yuan and Q. X. Yu, *Org. Biomol. Chem.*, 2010, **8**, 3618.
- 27 J. H. Song, M. X. Huai, C. C. Wang, Z. H. Xu, Y. F. Zhao and Y. Ye, *Spectrochim. Acta, Part A*, 2015, **139**, 549.
- 28 C. C. Wang, D. Zhang, X. V. Huang, P. G. Ding, Z. J. Wang, Y. F. Zhao and Y. Ye, *Sens. Actuators, B*, 2014, **198**, 33.
- 29 G. C. Li, G. Q. Gao, J. Y. Cheng, X. P. Chen, Y. F. Zhao and Y. Ye, *Luminescence*, 2016, **31**, 992.
- 30 J. Tang, S. G. Ma, D. Zhang, Y. Q. Liu, Y. F. Zhao and Y. Ye, *Sens. Actuators, B*, 2016, **236**, 109.
- 31 Y. Q. Ge, J. Jia, H. Yang, G. L. Zhao, F. X. Zhan and J. W. Wang, *Heterocycles*, 2009, **78**, 725.
- 32 Y. Q. Ge, A. K. Liu, J. Dong, G. Y. Duan, X. Q. Cao and F. Y. Li, *Sens. Actuators, B*, 2017, **247**, 46.
- 33 Y. Q. Ge, R. X. Ji, S. L. Shen, X. Q. Cao and F. Y. Li, *Sens. Actuators, B*, 2017, **245**, 875.
- 34 Y. Q. Ge, X. L. Zheng, R. X. Ji, S. L. Shen and X. Q. Cao, *Anal. Chim. Acta*, 2017, **965**, 103.

